Enthalpy Surfaces for Hydrogen Atom Transfer in a Molecular Crystal

V. A. Tikhomirov, A. V. Soudackov,† and M. V. Basilevsky*

Karpov Institute of Physical Chemistry, Vorontsovo Pole 10, 103064 Moscow, Russia

Received: January 27, 2000; In Final Form: November 5, 2000

The mechanism of the intermolecular photoinitiated hydrogen transfer in fluorene crystal doped with acridine molecules is studied theoretically. For this reaction, extensive experimental data in a wide interval of temperatures and pressures are available in the literature. Computations of energetics for this reaction with the explicit account of the crystalline environment are performed at atmospheric pressure, and also at 10 and 20 kbar. Parameters of the fluorene crystal lattice are reported as functions of pressure. The reaction model considers a large cluster of crystalline lattice arranged around the reaction pair; it includes three coordination spheres and its structure depends on pressure. The interaction inside the chemical subsystem is calculated by a semiempirical quantum-chemical method (PM3); its interaction with the crystalline environment is treated in terms of the atom−atom scheme. Studies of the potential energy surface (PES), as a function of pressure, showed that the tunneling transition of H-atom is essentially two-dimensional. Other modes that undergo a significant rearrangement and determine the reaction mechanism are revealed and investigated. The mechanism of multidimensional tunneling is discussed, and the computational scheme aimed at estimating the corresponding rate constant is outlined. It includes a computation of special PES cross sections providing relatively low effective potential barriers during the tunneling. The main visible effect of pressure on the PES is a significant decrease of equilibrium distances between reactants, promoted by increasing pressure. This results in decreasing the effective tunneling barriers along the reaction path and accelerating the reaction.

1. Introduction

A photochemical hydrogen transfer reaction between a fluorene molecule ($FluH_2$) in fluorene molecular crystal and excited triplet (T) acridine impurity (Ac) (scheme of reaction 1 is shown on Figure 1) inserted in this crystal has been thoroughly investigated experimentally during the past decade.[1−7]

$$Ac(T) + FluH_2 \rightarrow AcH + FluH \qquad (1)$$

As a primary step corresponding to scheme 1, two radical doublets are formed as products. The complete reaction mechanism is thoroughly discussed in the original literature[1]. Kinetics of stage 1 have been measured in a wide temperature (1.4−300 K) and pressure (1 atm − 35 kbar) range.[4−7] Because the size and shape of fluorene and acridine particles are very similar, it seems legitimate to consider the reacting system 1 as an ideal monocrystal. Thereby, it comprises a convenient model object for studying peculiarities of chemical reactions proceeding in molecular crystals.

The earlier quantum-chemical computations and other theoretical estimates[8−16] considered implicitly the influence of the crystalline environment on the reaction process. In the present work we compute potential energy surfaces (PESs) for reaction 1 with the environment corresponding to a real molecular crystal. Having, as a first stage, computed a structure of the crystalline lattice by standard methodologies,[17] we substitute one fluorene molecule by a triplet acridine and then calculate quantum-chemically a PES for the neighboring pair Ac(T) + $FluH_2$. Interactions of this system with the remainder of the crystal molecules during the course of reaction 1 are treated in terms of atom−atomic potential scheme.[17] Theoretical studies of similar type for other reactions in molecular crystals have been reported earlier.[18,19] Their extension to system 1 at ambient pressure has been performed recently.[20] Here we concentrate on the influence of external pressure on the reaction PES and proceed with a detailed analysis of the PES structure. Note that the corresponding pressure-dependent PESs are actually the enthalpy surfaces. The experimental data concerned with reaction 1 have been discussed recently at a phenomenological level[15,16] in terms of modern theories of reactive tunneling.[21] The present work provides relevant computational background for a consideration of this sort and also shows that several oversimplifications in the earlier treatment of the reaction mechanism must be eliminated. The detailed rate computations based on the PES analysis reported below are now in progress.

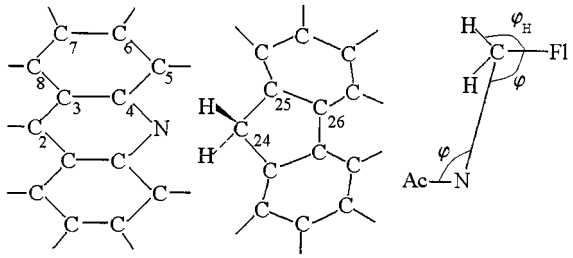

Figure 1. Scheme of reaction 1 in two projections. On the right-hand side, Ac and Fl denote acridine and fluorene fragments with their planes arranged perpendicular to the plane of the page.

2. Crystalline Structure

Basic crystallographic parameters optimized in the present computations are (a) three lattice parameters *a*, *b*, *c*; (b) three

* Corresponding author; E-mail: basil@cc.nifhi.ac.ru.
† Present address: Department of Chemistry and Henry Eyring Center for Theoretical Chemistry, University of Utah, Salt Lake City, UT 84112

10.1021/jp000334a CCC: $20.00
Published on Web 03/08/2001

TABLE 1: The Structure of the Fluorene Crystal under Different Pressures *P*

lattice parameters	1 bar experiment		calculations		
	[22]	[23]	1 bar	10 kbar	20 kbar
a	8.475	8.365	9.064	8.829	8.664
b	18.917	18.745	18.796	18.462	18.289
c	5.717	5.654	5.385	5.259	5.191
α	90.	90.	90.	90.	90.
β	90.	90.	90.	90.	90.
γ	90.	90.	90.	90.	90.
x		.1764	0.2250	0.2244	0.2239
y		.25	0.25	0.25	0.25
z		−0.0017	−0.1245	0.1248	−0.1250
φ		0.	0.	0.	0.
θ		56.0	51.6	52.2	52.7
ψ		0.	0.	0.	0.
d			1.229	1.287	1.332
H			−25.8	5.9	36.1

[a] Lengths of unit cells are given in Å, angles in degrees, energies in kcal/mol and densities in g/cm^3.

angles of the elementary cell α, *β*, *γ*; and (c) six parameters: *x*, *y*, *z* (coordinates of centers of mass) and *φ*, *θ*, *ψ* (Euler angles) specifying a position and an orientation of every symmetrically independent molecule in the unit cell. The experimentally determined values of these parameters supplemented by additional information (the type of a space group is *Pnma*, the number of the fluorene molecules in the unit cell $Z = 4$) for the fluorene crystal were used as input data. Williams−Starr[22] exp-6 parametrization of potentials was used for these calculations. Effect of pressure (*P*) was included by minimizing the enthalpy function

$$H = U + PV \tag{2}$$

where *U* is the potential energy and *V* is the volume of the unit cell.[23,24] Optimization of the structure in the frame of the space group *Pnma* and an alternative optimization of all parameters for every one of four molecules contained in a triclinic cell with the symmetry P1 yielded the same results, i.e., the symmetry *Pnma* is confirmed by the calculations.

The results of computations are listed in Table 1. At normal pressure (1 bar) the cell parameters are close to the experimental values.[25,26] These calculations (and all others) were performed using an equilibrium (PM3) geometry of fluorene. The empirical recommendation[22] to contract experimental C−H bond lengths by 0.07 Å did not substantially change the results. The structure of the fluorene crystal is shown in Figure 2 (actually, in Figure 2 one of the fluorene molecules is replaced with the acridine molecule). The calculations were made for the pressure range from 1 bar up to 20 kbar. In this range the crystal does not undergo phase transition[7] and its structure varies smoothly. The dependence of the volume of the unit cell on pressure is shown in Figure 3.

Practically, these calculations enable one, for a given pressure, to build clusters containing a sufficient amount of environment molecules and to insert the pair "acridine+fluorene" at the center of this cluster for the further investigation of the reaction 1.

The experimentally determined parameters of the fluorene crystal could be also used to build the cluster, but only for ambient pressure. The theoretical procedure described above provides consistently cluster structures within a wide pressure range when experimental data are unavailable.

3. Model Reaction System

The acridine impurity was modeled as follows. One of the fluorene molecules at the center of crystalline cluster was replaced by the acridine particle. Its position inside the cluster was optimized, minimizing the van der Waals interaction energy between this molecule and the rest of the cluster, the structure of which was now frozen during all calculations. The same Williams-Starr exp-6 potential, used in the modeling of the fluorene crystal, was applied in calculations, except the coulomb interactions, which were excluded due to their negligible effect as found at the preceding stage. Two different orientations of the guest acridine molecule in the host crystal are possible (see Figure 2). In both orientations the acridine molecule lies in the same plane, but the positions of the N−(reaction) center with respect to the transferring hydrogen atom are different. The geometry of the crystal is such that only one of these orientations is favorable for reaction 1. The minimum of the van der Waals energy was found for such favorable orientation of the acridine molecule. The importance of this configuration is independently supported by the experiment: the acridine impurities in the fluorene crystal were observed only with the "active" orientation for reaction 1.[2]

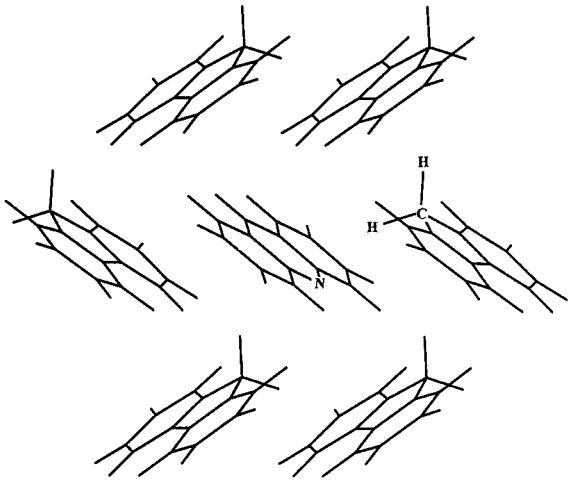

Figure 2. Fragment of the fluorene crystal with the acridine impurity substituted in the lattice for a fluorene molecule.

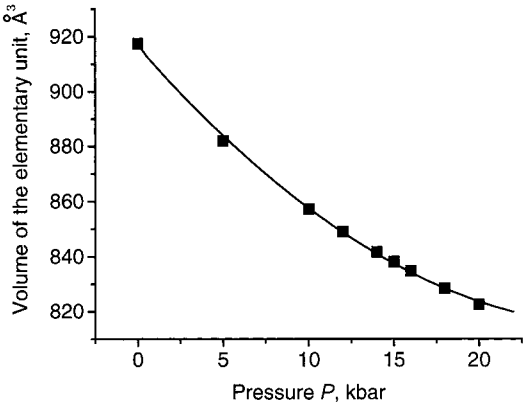

Figure 3. Pressure dependence for the unit cell volume of the fluorene crystal.

The acridine molecule with one of the neighboring fluorene molecules comprises a model of the reaction pair (1) inside the cluster. In practice, for the PES calculations, the reaction pair "fluorene+acridine" was inserted inside substituting for the pair of fluorene molecules withdrawn from the center of the cluster.

This pair and its cluster environment were further studied as a model of reaction 1. The potential energy surface was found as follows. Quantum-chemical calculations were performed for the reacting pair by semiempirical method PM3.[27] The influence

TABLE 2: Heats of the Reaction 1 (ΔH_r) and Barriers ($E^{\ddagger}$) (kcal/mol) and Basic Geometry Parameters for the Reagents (Re) and Products (Pr) of the Reaction 1 in the Fluorene Crystal under Different Pressures *P*

	$P = 1$ bar		$P = 10$ kbar		$P = 20$ kbar	
	Re	Pr	Re	Pr	Re	Pr
R_{eq}(CN)[a]	3.461	3.280	3.299	3.166	3.217	3.089
R(NH)[b]	2.492	0.995	2.356	0.995	2.271	0.995
R(CH)[b]	1.106	2.603	1.107	2.498	1.107	2.436
φ(AcNC)[c]	109.2	112.0	108.6	110.8	107.6	102.6
ΔH_r	−10.1		−10.4		−10.8	
$E^{\ddagger}$	21.6		21.6		21.7	

[a] Distances R are given in Å, angles in degrees. [b] Transferred atom H. [c] See Figure 1.

of the crystal was accounted as described above for the acridine molecule. It is displayed as an external potential field affecting both the structure of the pair and its position and orientation inside the cluster. The pressure dependence of this potential arises because of the pressure-induced change of the cluster structure. The main effect is revealed as a change of equilibrium distances in the pair of reactants. One can see from Table 2 that the equilibrium distance between the atoms C and N of the reaction center R_{eq}(CN) decreases considerably due to the increase of the pressure. The second effect is the change of the additional van der Waals interaction energy of the chemical system and the cluster under different pressures, which is controlled by the parameters of a cell (see Table 1).

4. PES Computations

The total potential energy U of system 1 in the crystal was computed as a sum of its PM3 total energy and the van der Waals interaction energy with the crystal. Full optimization of the internal coordinates of the reacting pair (1) as well as its position and orientation inside the cluster has been performed. The PM3 method gives satisfactory results in calculating heats of formation for a series of molecules similar to the reactants and the excitation energy of the acridine molecule. The calculated adiabatic value of the latter (T, π-type) is 1.77 eV, whereas the experiment gives the energy of the (π,π^*)-transition as 1.96 eV.[28] The calculated heat of reaction 1 in a vacuum is −9 kcal/mol, which is close to the value 7.6 kcal/mol used in ref 10.

Preliminary calculations for the gas phase and in crystal at ambient pressure[20] have revealed a specific relative arrangement of the reaction pair, forced by the crystal. The planes of reactant particles for their equilibrium configuration in the crystal are parallel, contrary to the gas phase in which they form a sharp dihedral angle. The barrier of the reaction in the crystal is higher than that in the gas phase: ∼22 kcal/mol vs ∼18 kcal/mol. The difference originates partly from an unfavorable orientation of the pair (2 kcal/mol) and partly from the increase of the van der Waals energy of the interaction of the reacting pair with the cluster (2 kcal/mol).

At a preliminary step of the PES investigation, we have identified the internal motions that are most important for the H-transfer in system 1. The values of the corresponding coordinates were found to be significantly different at reactant and product minima. These coordinates are listed in Table 3; we call them "reorganization modes". Also important are the modes that change significantly in the transition state (TS) region, although their reactant and product values are almost the same. We call them "promoting modes" and also include them in Table 3.

TABLE 3: Changes of Important Geometrical Parameters during the Course of Reaction 1 at Ambient Pressure[a]

$R(C_{24}-N)$	3.46 reagents	2.8 saddle point	3.28 product
	acridine fragment		
$N-C_4$	1.387	1.424	1.413
C_4-C_5	1.389	1.395	1.405
C_5-C_6	1.403	1.392	1.375
C_6-C_7	1.372	1.389	1.400
C_7-C_8	1.410	1.390	1.377
C_8-C_3	1.384	1.401	1.415
C_3-C_4	1.404	1.423	1.416
	fluorene fragment		
$C_{24}-C_{25}$	1.500	1.466	1.433
$C_{25}-C_{26}$	1.414	1.425	1.430
φ_H	121	149	180
φ	109	120	112

[a] Lengths in Å, angles in degrees. See Figure 1 for designation of geometrical variables.

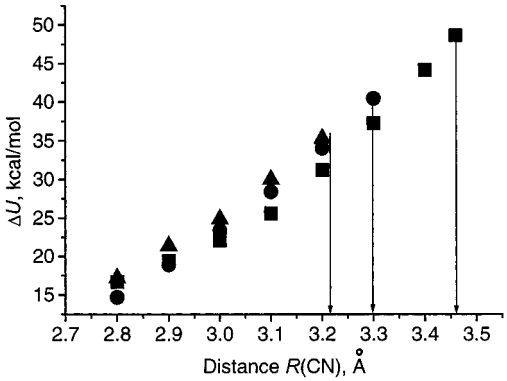

Figure 4. Barrier height $\Delta U(R)$ (eq 5) for different pressures. Vertical lines show the equilibrium for a given pressure value $R = R_{eq}$. Squares, $P = 1$ bar ($R_{eq} = 3.46$ Å); circles, $P = 10$ kbar ($R_{eq} = 3.30$ Å); triangles, $P = 20$ kbar ($R_{eq} = 3.22$ Å).

The most visible peculiarity of the reaction proceeding in a crystal, as compared to the gas-phase reaction, is a steric hindrance by the environment of mutual orientational motions in reactants. It gets stronger when pressure increases. Thereby, intermolecular orientational degrees of freedom become an essential ingredient of the reaction coordinate. The most important consequence is the fact that reaction in a crystal cannot be collinear. The motion of the transferred H atom is essentially two-dimensional.

Changes of important coordinates under pressure are shown in Table 2. The height of chemical reaction barriers and reaction heat effects are also shown.

The PES computations were performed at two levels of sophistication. First, we considered global minima and saddle TS points for system 1 in a crystal with a fixed single coordinate R, the distance between saturated C-atom of fluorene and N-atom of acridine in the reaction center C···H···N. This analysis implied full geometry optimization at fixed R. It provides the energy barrier $\Delta U(R)$ specified below (see eq 5) in more detail. Curves $\Delta U(R)$ for several pressures are shown in Figure 4.

The point corresponding to the minimum within the array of R-dependent TS points represents the classical global TS for system 1. Although, for reactions proceeding via tunneling regime, its kinetic importance is suppressed, this point is a conventional benchmark characteristic of the total PES. Its coordinates are almost independent of pressure: $R = 2.8$ Å, and heights of corresponding barriers are listed in Table 2.

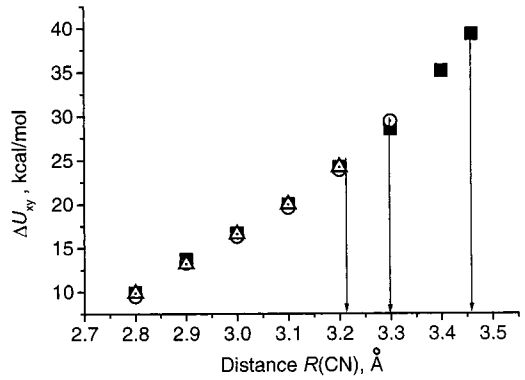

Figure 5. The barrier height $\Delta U_{xy}(R)$ (eq 6) for different pressures. Vertical lines and symbols are explained in Figure 4.

The second type of PES computations provided two-dimensional potential functions in terms of coordinates *x, y*, specifying a position of the transferred H-atom in the plane perpendicular to the planes of fluorene and acridine molecules and including atoms C and N of the reaction center (see Figure 1) These two-dimensional PESs, representing potentials governing reactive tunneling of H-atom, are also described below. They are functions of *R*, and the corresponding energy barriers $\Delta U_{xy}(R)$ (see eq 6 below) are shown in Figure 5.

5. Classification of Coordinates and Detailed PES Computations

Two basic reaction coordinates *x* and *y* define a position of the transferred H atom in the plane orthogonal to two planes in which the planar reactant molecules are kept (see Figure 1). The straight line connecting heavy atoms N and C of the reaction center lies in this plane. Next, the coordinates adjacent to the reaction center experience significant changes during a chemical rearrangement. Their basic origin is the change of hybridization states ($sp^3 \leftrightarrow sp^2$) of terminal atoms C and N of the reaction center. Thereby, the rearrangement modes are mainly hybridization ones; they are called *Q*-modes hereafter. Among promoting modes most important is *R*, a distance between the N atom of acridine and the C atom of the fluorene reaction center. The angular modes defining mutual orientation in the reacting pair, as discussed above, also belong to this category, although the corresponding energy changes are less than those accompanying changes of *R*. Their typical representative is symmetric internal rotation angle φ (see Figure 1). Altogether, we have a list of important coordinates: reaction coordinates: *x, y*; reorganization (hybridization) modes: *Q*; and promoting modes: *R*, φ.

We made an attempt to separate contributions of different classes of coordinates to the total PES. This is a necessary preliminary step before a rate calculation. The following procedure adopted for this purpose was based on three assumptions. (a) Coordinates *x, y* are "light" and fast; their dynamical rearrangement proceeds on a time scale which is much shorter than that for other ("heavy") modes. (b) Reorganization modes *Q* are slow. Their contribution to the rate can be described in terms of the Franck−Condon overlap integral between their initial and final states.[29,30] In the classical high-temperature limit, this Franck−Condon factor reduces to the usual Arrhenius exponential. (c) Heavy coordinate *R* is a single promoting mode. It can be considered as a parameter monitoring the reaction dynamics.

The corresponding computations proceeded in two steps.

Step 1. With fixed *R*, we found three stationary points of a PES by properly optimizing all other coordinates. The two minima and a saddle point obtained in this way are

$$U(x^r,y^r,Q^r|R)\text{: the reactant minimum}$$

$$U(x^p,y^p,Q^p|R)\text{: the product minimum}$$

$$U(x^{\neq},y^{\neq},Q^{\neq}|R)\text{: the saddle (TS) point.} \quad (3)$$

As functions of *R*, these points form three energy profiles, interpreted as bottoms of two (reactant and product) valleys and the TS ridge.

Step 2. With fixed *Q*-modes $Q = Q^{\neq}(R)$ we calculated two-dimensional PESs for reaction coordinates: $U(x,y|Q^{\neq}(R),R)$. They are called "reactive PESs" henceforth. Their stationary points are denoted as

$$U(x^r,y^r|Q^{\neq}(R),R)\text{: the reactant minimum}$$

$$U(x^p,y^p|Q^{\neq}(R),R)\text{: the product minimum}$$

$$U(x^{\neq},y^{\neq}|Q^{\neq}(R),R)\text{: the TS point} \quad (4)$$

Note that the TS points in the lists 3 and 4 coincide. These computations result in two *R*-dependent energy barriers.

$$\text{Step 1: } \Delta U(R) = U(x^{\neq},y^{\neq}|Q^{\neq}(R),R) - U(x^r,y^r,Q^r|R) \quad (5)$$

$$\text{Step 2: } \Delta U_{xy}(R) = U(x^{\neq},y^{\neq}|Q^{\neq}(R),R) - U(x^r,y^r|Q^{\neq}(R),R) \quad (6)$$

Equation 5 provides *R*-dependent barrier heights relative to the minima obtained by a full optimization of the reactant configuration with fixed *R*. Hybridization modes *Q* acquire their initial values at these minima. According to eq 6 reorganization modes (as well as other heavy modes) are fixed at their saddle point values, and only reactive coordinates *x, y* are relaxed to attain their minima. Actually, eq 6 represents the height of the barrier on the two-dimensional reactive PES, the main result of a computation at step 2 as described above.

The following simplified rearrangement mechanism underlies these computations. As a first step, the slow *Q*-modes change their configuration as $Q^r \rightarrow Q^{\neq}$. During this process, the fast *x, y* modes keep located at their minima adjusted for the change of *Q*. The corresponding energy consumption is

$$\Delta(R) = U(x^r,y^r|Q^{\neq}(R),R) - U(x^r,y^r,Q^r|R) \quad (7)$$

This quantity can be also considered as a contribution of *Q*-modes to the total reaction barrier at given *R*

$$\Delta(R) = \Delta U(R) - \Delta U_{xy}(R) \quad (8)$$

At the second step, the rearrangement of fast *x, y* modes takes place on the two-dimensional surface $U(x,y|Q^{\neq}(R),R)$. We expect it to proceed via the tunneling mechanism.

The corresponding rate constant can be estimated with a minimum effort for the high-temperature case, when coordinates *Q* and *R* are classical. Let us denote as $K_{xy}(R,T)$ the rate constant corresponding to the two-dimensional tunneling of hydrogen atom as described above. Then the total rate constant is

$$K(T) = \int \mathrm{d}R\, K(R,T) \exp\left(-\frac{V(R)}{k_B T}\right) \quad (9)$$

TABLE 4: Δ(*R*) Values (eq 8) as a Function of *R* at Different Pressure

	$R = 3.46$ Å	$R = 3.3$ Å	$R = 3.2$ Å	$R = 3.1$ Å	$R = 3.0$ Å	$R = 2.9$ Å	$R = 2.8$ Å
$P = 1$ bar	9.3	8.6	6.9	5.6	5.4	5.7	6.8
$P = 10$ kbar		11.0	10.1	8.8	7.1	5.6	6.6
$P = 20$ kbar			11.1	10.0	8.4	8.2	7.3

Here $V(R)$ is the energy profile along the reactant valley:

$$V(R) = U(x^r,y^r,Q^r|R) - U(x^r,y^r,Q^r|R_0) \qquad (10)$$

where $R_0 = R_{eq}$ corresponds to the global reactant minimum.

The R-dependent rate constant is defined as

$$K(R,T) = K_{xy}(R,T)\exp\left(-\frac{\Delta(R)}{k_B T}\frac{F_Q^{\ddagger}(R)}{F_Q^{r}(R)}\right) \qquad (11)$$

where $F_Q^{\ddagger}(R)$ and $F_Q^{r}(R)$ are the TS and reactant partition functions associated with Q-modes at the relevant PES points. It combines the contribution of both reaction and hybridization modes.

The algorithm suggested by eq 11 is similar to a standard prescription of the Golden Rule rate theory.[29,30] Classical modes contribute to the rate a TST-like factor with the Arrhenius temperature dependence multiplied by the tunneling transition rate due to quantum modes. This is valid on a purely harmonic PES composed of two intersecting paraboloids where noninteracting modes rearrange independently. We retain the same prescription for the PES of more complicated structure. Here a mode separation in the course of a transition is impossible. This is seen from the fact that the potential relief on which quantum tunneling of x, y modes occurs proves to be strongly Q-dependent. We consider only a transition at the saddle point $Q = Q^{\neq}(R)$, which gives the main contribution to the total reaction rate. This point is obviously a counterpart of a quasi-intersection point on a two paraboloid PES of the nonadiabatic Golden Rule model. Thereby, eq 11 comprises a reasonable extrapolation of the principles of the harmonic rate theory, summarized as items (a)−(c) above, for PESs which are essentially anharmonic. A fully consistent account of anharmonicity would not allow for mode separation; it requires to consider a multidimensional tunneling in the full x, y, Q space.

6. Results and Discussion

A. Pressure Dependence of Basic PES Characteristics. The increase of pressure promotes the energy increase which is a combination of two contributions:

$$U = U_{chem} + U_{vdw} \qquad (12)$$

This equation corresponds to the computational procedure as described in section 3; here U_{chem} represents the result of PM3 computation for a given geometry of the reacting system 1, and U_{vdw} is the atom−atom interaction energy between the chemical system 1 and the frozen (at given pressure) crystalline environment. The last term depends on a position and orientation of the chemical system in the cavity inside the crystal and is optimized relative to the corresponding variables. Both terms in eq 12 increase with the growth of pressure: for the first term this is a result of growing nonequilibrium shift for relevant system internal coordinates, whereas the second term obviously increases due to repulsion effects within a cavity which is compressed and decreases in volume.

The calculated energetics is nearly independent of pressure, for instance, such are the global barrier height $\Delta U^{\neq}$ and heat of reaction (see Table 2). The same is true for R-dependent barriers (eq 5), which are illustrated by Figure 4 and, as can be seen, depend very slightly on pressure. The tunneling barriers (eq 6) for different pressures practically coincide within optimization errors (Figure 5). The most important effect of the pressure consists of shortening the equilibrium separation R_{eq} of the reacting particles. Figures 4 and 5 illustrate this fact. Because R_{eq} decreases, for given R the same barrier $\Delta U_{xy}(R)$ (Figure 5) becomes energetically more easily accessible with the stronger pressure. This is in accord with the experimental data indicating that the reaction rate grows exponentially when pressure increases.[4−7]

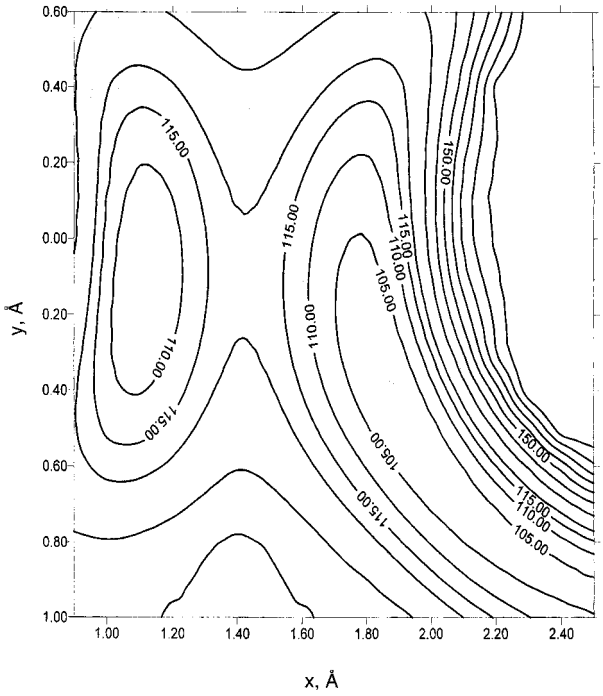

Figure 6. A map of a typical PES $U(x_r,y_r|Q^{\neq}(R),R)$ displaying the tunneling landscape. H-atom coordinates x and y are defined in the text at the end of section 4. The origin of the coordinate frame coincides with the C-atom of the fluorene reaction center. The constant energy contours are given in kcal/mol.

B. Two-Dimensional Reactive PESs. The reactive PESs $U(x,y|Q^{\neq}(R),R)$ calculated as described in section 5 (Step 2) are the main computational outcome of the present work. They comprise a necessary background for future computations of tunneling amplitudes and reaction rates. The typical PES is shown on Figure 6. Its shape provides an apparent illustration of the statement that H-transfer is not collinear. The barrier heights shown in Figure 5 correspond to the saddle points of such PESs. Note that because the tunneling is two-dimensional, they provide the lower bound for effective reaction barriers.

C. Hybridization *Q* Modes. Specification of Q-modes and their contribution to the energy barriers is a necessary preliminary step prior to a computation of reactive PESs. The corresponding ingredient of the barrier height is the quantity $\Delta(R)$ described by eqs 7 and 8. Provided Q-modes are classical (the high-temperature limit) their effect on the reaction rate can be treated in terms of eqs 9−11; the quantum kinetic effect of

Q-modes is introduced in terms of their Franck−Condon factor,[29,30] a quantity also strongly dependent on $\Delta(R)$.

The values of $\Delta(R)$ listed in Table 4 confirm the significance of explicit consideration of *Q*-modes. Their role has been practically neglected in the earlier interpretations of reaction kinetics for system 1. So, the barrier heights pertaining to the tunneling computations, as suggested according to the earlier quantum-chemical approaches,[8] seem to be too high (by several kcal/mol), which is expected to strongly exaggerate tunneling effects. This becomes most transparent from a consideration of the H/D kinetic isotope effect for which tentative estimates[15,16] predicting a retardation of the reaction including deuterium by 4−8 orders of magnitude, are incompatible with the measured values[7] showing much lower effect.

Conclusion

In the present work, we report quantum-chemical PM3 calculations of PESs for hydrogen transfer photo reaction with account for the crystalline environment. The pressure effect is explicitly introduced in a PES computation via a contraction of characteristic lengths of the crystalline lattice and the resulting increase of the interaction (repulsion) energy between the environment molecules and the reacting system. The computation provides both basic conventional characteristics of the global PES (coordinates and relative energies of its stationary points) and also detailed information required for the forthcoming computations of reaction rates with account of reactive tunneling. The importance of changes of hybridization modes as an essential element of the reaction mechanism is emphasized and quantitatively demonstrated.

Acknowledgment. The authors are grateful to L. I. Trakhtenberg for stimulating discussions and A. V. Dzjabchenko for providing the code for regular computations of molecular crystals. The work was supported by RFBR Grants 00-15-97295 and 99-03-33196 and by INTAS-RFBR Grant 97-IR-620.

References and Notes

(1) Prass, B.; Colpa, J. P.; Stehlik, D. *J. Chem. Phys*. **1988**, *88*, 191.
(2) Prass, B.; Colpa, J. P.; Stehlik, D. *Chem. Phys.* **1989**, *136*, 187.
(3) Prass, B.; Colpa, J. P.; Stehlik, D. *Chem. Phys.* **1989**, *136*, 187.
(4) Bromberg, S. E.; Chan, I. Y.; Schilke, D. E.; Stehlik, D. *J. Chem. Phys.* **1993**, *98*, 6284.
(5) Chan, I. Y.; Wong, Ch. M.; Stehlik, D. *Chem. Phys. Lett.* **1994**, *219*, 187.
(6) Chan, I. Y.; Dernis, M. S.; Wong, Ch. M.; Prass, B.; Stehlik, D. *J. Chem. Phys.* **1995**, *103*, 2959.
(7) Chan, I. Y.; Hallock, A. J.; Prass, B.; Stehlik, D. *J. Phys. Chem. A* **1999**, *103*, 344.
(8) Flomenblit, V. Sh.; Mikhejkin, I. D.; Trakhtenberg, L. I. *Dokl. Akad. Nauk Phys. Chem.* **1991**, *320*, 922 (in Russian); 695 (in English).
(9) Chantranupong, L.; Wildman, T. A. *J. Chem. Phys.* **1991**, *94*, 1030.
(10) Lavtchieva, L.; Smedarchina, Z. *Chem. Phys. Lett.* **1991**, *184*, 545.
(11) Lavtchieva, L.; Smedarchina, Z. *Chem. Phys. Lett.* **1991**, *187*, 506.
(12) Lavtchieva, L.; Smedarchina, Z. *Chem. Phys.* **1992**, *160*, 211.
(13) Trakhtenberg, L. I.; Flomenblit, V. Sh. *Russ. J. Phys. Chem.* **1993**, *67*, 1464.
(14) Flomenblit, V. Sh.; Trakhtenberg, L. I. *Chem. Phys. Rep.* **1994**, *11*, 1931.
(15) Trakhtenberg, L. I.; Klochikhin, V. L. *Chem. Phys.* **1998**, *232*, 175.
(16) Prass, B.; Stehlik, D.; Chan, I. Y.; Trakhtenberg, L. I.; Klochikhin, V. L. *Ber. Bunsen-Ges. Phys. Chem.* **1998**, *102*, 498.
(17) Pertsin, A. J.; Kitaigorodsky, A. I. *The atom−atom potential method.* Springer Verlag: Berlin, 1987.
(18) Basilevsky, M. V.; Gerasimov, G. N.; Petrochenko, S. I.; Tikhomirov, V. A. *Chem. Phys.* **1981**, *55*, 259.
(19) Basilevsky, M. V.; Gerasimov, G. N.; Petrochenko, S. I. *Russ. Chem. Phys.*, **1984**, *3*, 162.
(20) Tikhomirov, V. A.; Soudackov, A. V.; Basilevsky, M. V.; Trakhtenberg, L. I. *Russ. J. Phys. Chem*. **1999**, *73*, 332.
(21) Goldanskii, V. I.; Trakhtenberg, L. I.; Fleurov, V. N. Tunneling phenomena in chemical physics; Gordon and Breach Science: New York, 1989.
(22) Williams, D. E.; Starr, T. H. *Comput. Chem.* **1977**, *1*, 173.
(23) Basilevsky, M. V.; Weinberg, M. M.; Dzjabchenko, A. V. *Dokl. Akad. Nauk Phys. Chem.* **1984**, *277*, 384 (in Russian).
(24) Dzjabchenko, A. V.; Basilevsky, M. V. *Russ. J. Struct. Chem.* **1985**, *26*, 72.
(25) Belsky, V. K.; Zavodnik, V. E.; Vozzhennikov, V. M. *Acta Crystallogr*. **1984**, *C40*, 1210.
(26) Gerkin, R. E.; Lundstedt, A. P.; Reppart, W. J. *Acta Crystallogr., Sect C (Cr. Str. Comm.)* **1984**, *40*, 1892.
(27) Stewart, J. J. P. *J. Comput. Chem.* **1989**, *10*, 209.
(28) McGlinn, S. P.; Azumi, T.; Kinoshito, M. *Molecular spectroscopy of the triplet state*; Prentice Hall, Inc.: Englewood Cliffs, New Jersey, 1969.
(29) Dogonadze, R. R.; Kuznetsov, A. M. *Itogi nauki i techn. Ser. Phys. Chem., Kinet.*; VINITI: Moscow, 1973; Vol.2.
(30) Ulstrup, J. *Charge transfer in condensed media*; Springer-Verlag: Berlin, 1979.